Available online at www.sciencedirect.com

ScienceDirect

Ceramics International 40 (2014) 4311–4317

CERAMICS INTERNATIONAL

www.elsevier.com/locate/ceramint

The effect of Ga^{3+} addition on the sinterability and microwave dielectric properties of $RE_3Al_5O_{12}$ (Tb^{3+}, Y^{3+}, Er^{3+} and Yb^{3+}) garnet ceramics

Annrose Sunny, Varsha Viswanath, Kuzhichalil Peethambharan Surendran, Mailadil Thomas Sebastian*

Materials Science and Technology Division, National Institute for Interdisciplinary Science and Technology, CSIR, Thiruvananthapuram 695019, India

Received 22 June 2013; received in revised form 22 August 2013; accepted 22 August 2013
Available online 4 September 2013

Abstract

The $RE_3Al_5O_{12}$ (RE = Tb, Y, Er, Yb) ceramics have been prepared by the mixed oxide route and the influence of Ga^{3+} doping on their properties is investigated. The intrinsic $Y_3Al_5O_{12}$ (YAG) ceramic sintered at 1650 °C for 4 h showed good dielectric properties; ($\varepsilon_r = 10.1$, $Q_u \times f = 65{,}000$ GHz, $\tau_f = -45$ ppm/°C). Addition of Ga_2O_3 was found to be beneficial in improving the densification of $Tb_3Al_5O_{12}$, $Er_3Al_5O_{12}$ and $Yb_3Al_5O_{12}$ except $Y_3Al_5O_{12}$ where Nb_2O_5 is the better choice. Among Ga^{3+} added samples, the composition $Yb_3Al_5O_{12} + 1$ wt% Ga_2O_3 showed good microwave dielectric properties: $\varepsilon_r = 10.3$, $Q_u \times f = 50{,}000$ GHz, $\tau_f = -58$ ppm/°C. The $Y_3Al_5O_{12}$ doped with 1 wt% Nb_2O_5 has $\varepsilon_r = 10.7$, $Q_u \times f = 120{,}000$ GHz and $\tau_f = -45$ ppm/°C. The ceramics have good thermal properties (CTE = 2–3 ppm/°C, $\lambda = 2$–12 W/m K).

Keywords: A. Sintering; Ceramics; Garnets; Microwave dielectrics; Densification

1. Introduction

With the emergence of mobile communication revolution, the low loss dielectric ceramics find huge demands as resonators in antennas, filters, oscillators and also as substrates in microwave electronic gadgets. These applications rely on the low loss nature and low permittivity of the dielectric ceramics. Moderately high permittivity ($\varepsilon_r > 20$) materials are required for microwave resonator application in order to facilitate miniaturization since the electrical performance of circuits and devices is highly dependent on the permittivity ε_r of the dielectric medium. On the other hand low permittivity ($\varepsilon_r < 15$) materials are mainly used for substrate applications. The low permittivity ceramics maximize the signal propagation speed through the substrate and minimize the cross coupling effect with conductors [1]. The other major requirement for substrate applications are high quality factor ($Q_u \times f$), low temperature coefficient resonant frequency (τ_f), low value of linear coefficient of thermal expansion (CTE), and high thermal conductivity (λ) [1,2].

Silicates and aluminates are found to be promising materials for substrate applications due to their low relative permittivity [3–5]. Perovskite type aluminates and gallates are widely used as substrate materials for epitaxy of HTSC and CMR materials [4]. Over the last few decades, several rare earth substituted aluminates and silicates have been reported for microwave substrate applications [5,6]. However, the high processing temperature limits their wider acceptance due to the extra cost factor involved. A brief survey of literature reveals that the addition of low melting glasses and sintering aids (LMZBS, LBS, ZBS, Ga_2O_3, ZrO_2, LiF, TeO_2, V_2O_5, CuO) which improve the relative density of ceramic samples via liquid phase sintering at low temperatures without considerably affecting the dielectric properties [5,7–9].

Garnets are well known material for solid state lasers, microwave resonators, and thin film substrates in electronic module [10]. Rare earth aluminum garnets and their derivatives offer several important technological applications [11]. Rare earth garnets having general formula $R_3M_5O_{12}$, (R is the rare earth element or yttrium and M = Al, Fe, Ga etc.) belong

---

*Corresponding author. Tel.: +91 4712515294.
E-mail address: mailadils@yahoo.com (M. T. Sebastian).

0272-8842/$ - see front matter © 2013 Elsevier Ltd and Techna Group S.r.l. All rights reserved.
http://dx.doi.org/10.1016/j.ceramint.2013.08.097

to the hexaoctahedral class of cubic structure with $Ia\overline{3}d$ space group [12]. Several authors attempted to investigate the structure–property relation of these garnets. For example, the chemical bond formation and hardness estimation of rare earth garnets has been studied by Gao et al. [13]. Hosokawa et al. reported the thermodynamical instability of rare earth garnets of high ionic radii [14].

$Y_3Al_5O_{12}$ (YAG) is obviously a well studied material in this family. Despite the enormous applications of YAG materials in laser electronics, synthesis and development of coherently dense YAG has been a challenge. Recently Vlasova et al. reported the laser synthesis of YAG ceramics from powder mixtures of Y_2O_3–Al_2O_3 ceramics [15]. However, the microwave loss properties of these materials were largely unexplored until 2009, when Kagomiya et al. reported that the polycrystalline YAG ceramic sintered at 1650 °C for 24 h offered very high densification (99%), exceedingly high quality factor ($Q_u \times f = 440{,}000$ GHz), and relative permittivity of about 10.5 with a τ_f of -66 ppm/°C [16]. However, subsequent studies by other groups could not generate this high quality factor in YAG. For example, Zhou et al. reported that YAG ceramic doped with TiO_2 showed much inferior microwave dielectric properties ($\varepsilon_r = 10.2$, $Q_u \times f = 80{,}100$ GHz, $\tau_f = -30$ ppm/°C) but at a lower sintering temperature of 1150 °C/4 h [17]. On the other hand, the YAG single crystal with garnet structure showed a quality factor 10,50,000 GHz [11]. Evidently, the factors′ controlling dielectric loss mechanism in rare earth aluminate garnets with $Y_3Al_5O_{12}$ in particular, is not well understood. Selection of an ideal dopant or sintering aid for a peculiar microwave dielectric ceramic has been very tricky where key aspects of partial substitution as well as liquid phase sintering have to be considered. Even though the action of a dopant will vary from material to material, there are several reports on the effect of Ga_2O_3 in improving the microwave dielectric properties, in different microwave ceramic systems. For example, Yang et al. in 2002 reported that Ga_2O_3 is an ideal choice to improve the sintering behavior thereby resulting in the enhancement of density and microwave dielectric properties of a $Ba(Zn_{1/3}Ta_{2/3})O_3$ ceramic [18]. Shirey and Feteira was also found that Ga_2O_3 is a useful sintering aid in other systems like $Ba(Mg_{1/3}Ta_{2/3})O_3$ [19], $BaTiO_3$ [20] etc. Hence the present study investigates the effect of trivalent (Ga^{3+}) dopant in rare earth garnets $RE_3Al_5O_{12}$ (RE=Tb, Y, Er, Yb) on their sintering behavior (densification) and microwave dielectric properties.

2. Experimental procedure

The conventional solid state ceramic route was employed for the preparation of $RE_3Al_5O_{12}$ (RE=Tb, Y, Er, Yb) ceramics. High purity powders of Tb_2O_3, Y_2O_3, Er_2O_3 and Yb_2O_3 (99.9%, IRE, India), Al_2O_3 (99.9%, Sigma-Aldrich, USA) were stoichiometrically weighed and ball milled using zirconia balls in ethanol for 24 h. The ceramic powders were calcined at 1250 °C for 4 h. 1 wt% Ga_2O_3 ($\geq 99.99\%$, Sigma-Aldrich, USA) were added to the fine powder of calcined ($Tb_3Al_5O_{12}$) TbAG, ($Y_3Al_5O_{12}$) YAG, ($Er_3Al_5O_{12}$) ErAG and ($Yb_3Al_5O_{12}$) YbAG. 4 wt% Poly Vinyl Alcohol (PVA) (molecular weight 22,000, BDH Lab Suppliers, UK) solution was then added to it and mixed. It was then dried, ground well and pressed into cylindrical disks of various dimensions for microwave dielectric (diameter = 11 mm, thickness = 3–4 mm), linear thermal expansion (diameter = 8 mm, thickness = 10 mm) and thermal conductivity (diameter = 12.6 mm, thickness = 1.8 mm) measurements. The sintering of the rare earth garnet was carried out in the temperature range 1400–1650 °C for 4 h.

The sintered and powdered samples were used to analyze the crystalline structure and phase purity by the X-ray diffraction technique using Ni filtered CuKα radiation (PANalytical X′ Pert PRO Diffractometer, Netherlands). The microstructures of the sintered samples were studied using scanning electron microscope (JEOL-SEM 5601v, Tokyo, Japan). The samples were polished well and thermally etched for 30 min at a temperature 50 °C below the sintering temperature. The surface of thermally etched sample was coated with a thin layer of gold prior to SEM analysis. The sintered densities of the specimen were measured by the Archimedes method. The microwave dielectric properties were measured in the frequency range of 5–15 GHz using a Vector Network Analyzer (E5071C, Agilent Technologies, USA). The relative permittivity of the material was measured using Hakki–Coleman technique modified by Courtney. The TE_{011} mode was used for this measurement [21]. The unloaded quality factor (Q_u) was measured using $TE_{01\delta}$ mode by the cavity method [22]. The temperature variation of resonant frequency (τ_f) was measured by noting the temperature at regular intervals of 5 °C in the course of heating and was calculated using the equation [23].

$$\tau_f = \frac{1}{f_0}\frac{\Delta f}{\Delta T} \tag{1}$$

where f_0 is the resonant frequency at room temperature, Δf is the variation in resonant frequency and ΔT is the corresponding difference in temperatures. The thermal diffusivity (α) of the sintered samples were measured in the room temperature using Laser Flash Thermal Properties Analyzer (Flash Line 2000, Anter Corporation, USA). Thermal conductivity (λ) was then calculated using the equation [24],

$$\lambda = \alpha \rho C_p \tag{2}$$

where C_p is the specific heat capacity and ρ is the density of the material. The linear coefficient of thermal expansion (CTE) of the ceramic sample was measured using dilatometer (DIL 402 PC, NETZSCH, Germany) in the temperature range 30–500 °C. CTE was calculated using the equation [23].

$$\mathrm{CTE} = \frac{1}{L}\frac{\Delta L}{\Delta T} \tag{3}$$

where L is the length of the material, $\Delta L/\Delta T$ is the change in length per unit change in temperature.

3. Results and discussion

Garnet is one of the most studied materials due to their enormous potential as a host material in solid state lasers. The powder XRD patterns of $RE_3Al_5O_{12}$, (RE=Tb, Y, Er, Yb) sintered in the range 1550–1650 °C/4 h are shown in Fig. 1. The cubic unit cell of a general garnet compound $A_3B'_2B''_3O_{12}$ contains eight formula units. It has a bcc structure (space group $la\bar{3}d$ or O_{10}^h) with 160 (80) atoms in the primitive cubic cell. Usually the RE^{3+} ions occupy the 24(c) sites and each are dodecahedroally coordinated to eight O. The O^{2-} anions occupy the 96(h) sites whose exact locations depend on three structural parameters x, y, and z. There are two different sites for Al^{3+}, Al_{oct} (B' ion) occupy the 16(a) site with octahedral point symmetry (C_{3i}) and Al_{tet} (B'' ion) occupy the 24(d) sites with tetrahedral point symmetry ($S4$). In short, the $RE_3Al_5O_{12}$ garnet structure can be viewed as interconnected octahedraons, tetrahedrons, and dodecahedrons with shared O atoms at the corners [25]. The peaks are indexed using the JCPDS file no. 76-0111, which belongs to cubic rare earth garnets with $la\bar{3}d$ [no. 230] space group. From Fig. 1 it is obvious that the XRD patterns of all the compositions are similar with an expected shift in peak positions due to the gradual decrease in the ionic radius of RE^{3+} ions [26]. A similar periodic shift in peak positions with decrease of ionic radius of the RE^{3+} cation and subsequent shrinkage of the unit cell was observed in several other low loss rare earth based systems such as $RETiTaO_6$ [27] and $Sr_2(RE, Nb)O_6$ [28]. As part of the present investigation we have synthesized several other rare earth aluminate garnets based on $RE_3Al_5O_{12}$ (RE=Pr, Nd, Sm, Gd, Dy) but are found to be crystallizing in a polyphasic structure as a mixture of $REAlO_3$ and Al_2O_3. A previous report on the sol–gel synthesis method for the preparation of garnet crystal structure concluded that the rare earth aluminate garnets with high ionic radii are unstable and is stable only with RE=Gd–Lu [29]. However, Garskaite et al. in 2007 reported that $Eu_3Al_5O_{12}$ (EAG) also crystallizes in stable cubic garnet structure when synthesized through aqueous sol–gel process [30].

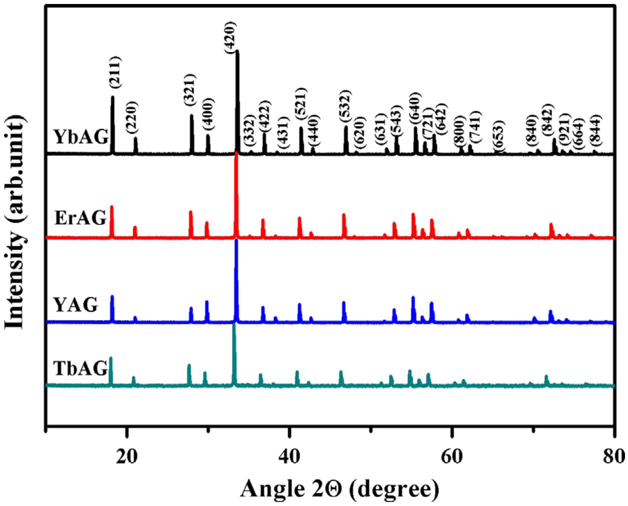

Fig. 1. The powder XRD patterns of (a) $Tb_3Al_5O_{12}$ (TbAG) sintered at 1575 °C for 4 h, (b) $Y_3Al_5O_{12}$ (YAG) sintered at 1650 °C for 4 h, (c) $Er_3Al_5O_{12}$ (ErAG) sintered at 1600 °C for 4 h and (d) $Yb_3Al_5O_{12}$ (YbAG) sintered at 1650 °C for 4 h.

It is well proven that the microwave dielectric properties of the ceramic are intimately related to its microstructure. A dense, defect free microstructure may largely improve the dielectric properties [31]. The SEM images of $Er_3Al_5O_{12}$ sintered at 1600 °C/4 h, $Er_3Al_5O_{12}+1$ wt% Ga_2O_3 sintered at 1550 °C/4 h, $Yb_3Al_5O_{12}$ sintered at 1650 °C/4 h and $Yb_3Al_5O_{12}+1$ wt% Ga_2O_3 sintered at 1600 °C/4 h are shown in Fig. 2(a), (b), (c) and (d). The microstructure of the undoped specimens (see Fig. 2(a) and (c)) shows polygonal grains of varying sizes with poor close packing due to poor densification (ErAG (90%) and YbAG (88%)). For ErAG, grain size varies from 1 to 3 μm (Fig. 2a). For YbAG grain sizes are in the

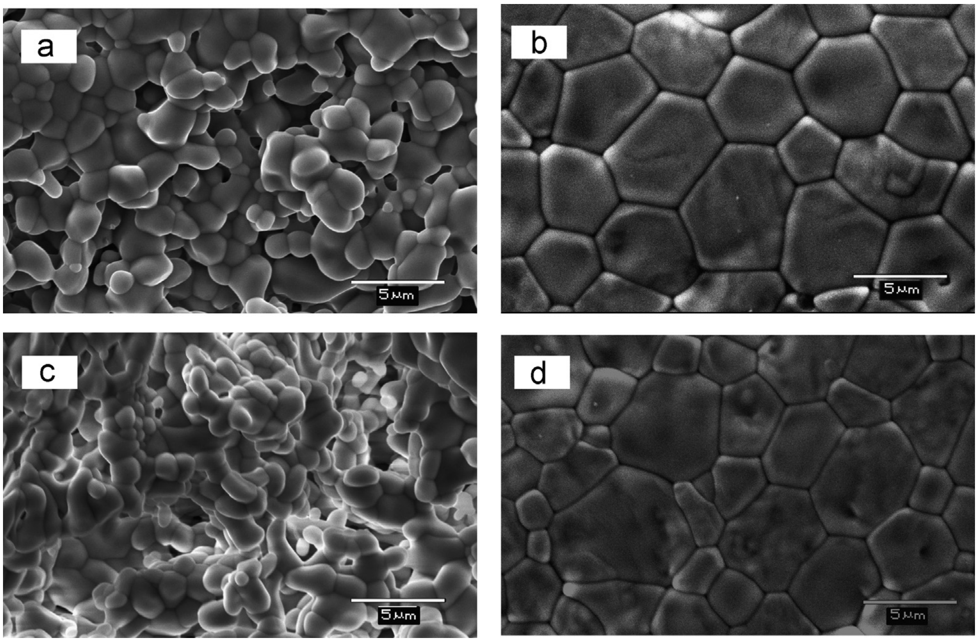

Fig. 2. SEM image of (a) $Er_3Al_5O_{12}$ sintered at 1600 °C/4 h, (b) $Er_3Al_5O_{12}+1$ wt% Ga_2O_3 sintered at 1550 °C for 4 h, (c)$Yb_3Al_5O_{12}$ sintered at 1650 °C/4 h and (d) $Yb_3Al_5O_{12}+1$ wt% Ga_2O_3 sintered at 1600 °C for 4 h.

Table 1
Total ionic polarizability, cell volume, sintering temperature, relative density, microwave dielectric properties and thermal properties of rare earth garnet ceramics.

Material	Total ionic polarizability (Å)^3	Cell volume (Å)^3	Sintering temp. (°C)	Relative density (%)	Apparent ε_r	$Q_u \times f$ (GHz)	τ_f (ppm/°C)	Apparent T_c (W/m K)	Porosity corrected T_c (W/m K)	CTE (ppm/°C)
$Tb_3Al_5O_{12}$	40.52	220	1575	92	10.7	13,400	−66	05.0	5.43	2.86
$Y_3Al_5O_{12}$	39.38	216	1650	96	10.6	65,000	−45	12.6	12.90	2.13
$Er_3Al_5O_{12}$	39.39	215	1600	90	10.5	11,700	−45	02.6	2.80	2.83
$Yb_3Al_5O_{12}$	38.64	213	1650	88	10.3	12,900	−70	02.0	2.27	2.41

range 0.5 to 2 μm (Fig. 2c). From Fig. 2(b) and (d) it can be seen that the Ga_2O_3 added ErAG and YbAG ceramics show a relatively dense microstructure with uniform equiaxed grain structure. It is also noteworthy that there is a decrease in grain size when Er is replaced with Yb (Fig. 2). Furthermore, despite the Ga_2O_3 doping, the micrographs do not reveal any secondary phase formation in ErAG and YbAG (Fig. 2(b) and (d)) which gives a clear indication that Ga_2O_3 doping is effective in bringing about densification in garnets through liquid phase sintering or through defect chemistry enhanced densification mechanism.

Table 1 gives the sintering temperature, relative density, microwave dielectric and thermal properties of the series of rare earth garnets. Interestingly, as the size of the cation decreases from Tb^{3+} to Yb^{3+} the sintering temperature increases while the relative density decreases (with the exception of YAG). From the present investigation, it is revealed that most of the rare earth aluminate garnets have poor densification in the intrinsic form. For example, relative density of $Er_3Al_5O_{12}$ is only 90% at sintering temperature of 1600 °C/4 h while in the case of $Yb_3Al_5O_{12}$ it is 88% when sintered at 1650 °C/4 h. The different trend is observed in $Y_3Al_5O_{12}$ (YAG) which shows 96% of its theoretical density at a relatively high sintering temperature of 1650 °C/4 h.

According to Claussius–Mossotti equation, the dielectric permittivity largely depends on the ionic polarizability. The permittivity of garnets was evaluated using the polarizability and cell volume. Table 1 also gives the total ionic polarizability (α_D), cell volume, quality factor ($Q_u \times f$) and the temperature coefficient of resonant frequency (τ_f) of pure rare earth garnet ceramics. Since the ionic radius of the cation decreases from Tb^{3+} to Yb^{3+}, obviously the unit cell volume also decreases. The total ionic polarizabilities of individual material (see Table 1) are calculated from the individual ion polarizabilities [23]. The α_D of the material shows a linear trend with the ionic radii of the rare earth ions (Tb, Y, Er, Yb). The molecular polarizabilities of YAG and ErAG are close to each other which is due to the fact that both Y and Er show similar ionic poarizabilities [23]. The apparent ε_r value are also given in Table 1, the values are in the range 10.3–10.7. The variation of ε_r decreases with decrease in the ionic radii of rare earth elements. The $Q_u \times f$ values of individual ceramics vary between 12,000 GHz and 65,000 GHz. One among the reason for the low value of $Q_u \times f$ for the pure rare earth garnets may be due to the low relative density of the samples. The intrinsic structural parameters like anharmonicity in the interaction between the electric field with the phonon system of the dielectric and extrinsic factors like porosity, impurities and random crystalline orientations affect the quality factor of the ceramics [32]. One of the effective way to improve densification and hence the quality factor is by aliovalent doping which is being undertaken in this study. The τ_f value of the garnet ceramics vary between −45 ppm/°C and −70 ppm/°C.

Table 1 also summarizes the thermal conductivity (λ) of rare earth garnet ceramics. The λ values vary in the range 2–12 W m^{-1} K^{-1}. Essentially thermal conductivity is a measure of the ability of a material to dissipate heat from the ceramic substance. The high λ (12 W/m K) of YAG may be a desirable feature in microelectronic substrates and packages where high thermal conductivity materials are of great demand, as a means to dissipate the heat generated in microelectronic circuits. The thermal conductivity depends on the composition, structure, defect state, temperature and microstructural features such as porosity, cracks and second phases of the material [22]. The effect of porosity on the λ values can be minimized by calculating the porosity corrected λ values using the following equation [32].

$$\lambda(\text{corrected}) = \frac{\lambda}{1-P} \qquad (5)$$

where P is the fractional porosity computed from the apparent and X-ray densities. The values of λ (corrected) obtained for $RE_3Al_5O_{12}$ is given in Table 1. The porosity corrected λ decreases when Tb^{3+} is replaced with Er^{3+} and Yb^{3+} in rare earth aluminate garnet structure. This may be due to a more inelastic phonon scattering resulting from the substitution and the subsequent reduction in phonon mean free path [28]. The $Y_3Al_5O_{12}$ shows very high λ value, this may be due to the fact that YAG is less porous (relative density = 96%) at 1650 °C/4 h compared to other rare earth garnets. All of the ceramics in this investigation showed a low CTE (<3 ppm/°C) (Table 1), and is comparable with the CTE value of silicon which is one of the desirable properties for their suitability as microwave substrates [3,32].

Fig. 3 shows the variation of lattice parameter and measured relative permittivity of gallium oxide added garnet composition as a function of ionic radius of rare earth elements. The ionic radius of the rare earth ion is taken from R.D. Shannon with 6 as the coordination number [33]. The lattice parameters of TbAG, YAG, ErAG and YbAG are calculated from the XRD pattern by graphical extrapolation using Nelson–Riley function [26]. The values obtained are $a = 12$ Å for TbAG, 12.02 Å for YAG, 11.96 Å for ErAG and 11.93 Å for YbAG. In the case of YAG, a marginal increase in the lattice parameter is observed, which can be understandable since Yttrium is lighter than the rest of the rare earth elements and does not belong to the lanthanide group. The measured value of ε_r for the Ga_2O_3 added garnet ceramic composites decrease with decrease in ionic radii of rare earths and it varies between 10.3 and 10.9 monotonously as a function of the ionic radius of rare earth elements.

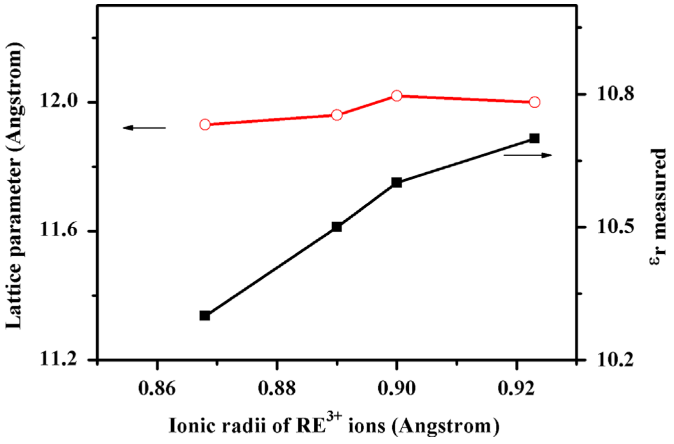

Fig. 3. The variation of lattice parameter and ε_r measured of $RE_3Al_5O_{12}$ (RE=Tb, Y, Er, Yb) garnet ceramics as a fuction ionic radius of RE^{3+} ions.

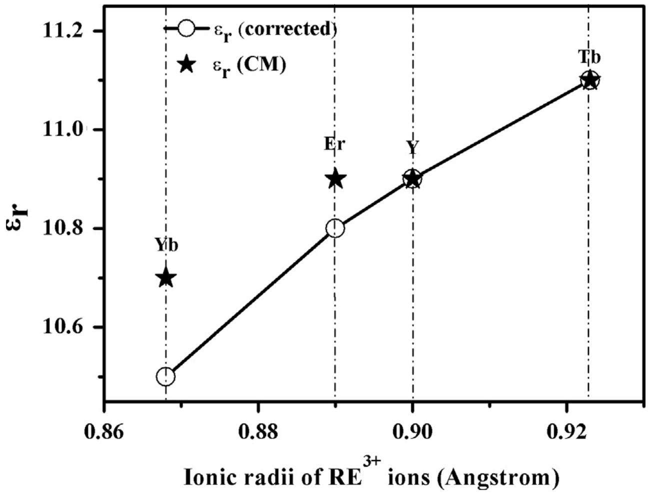

Fig. 4. The variation of ε_r (corrected) and ε_r (CM) of $RE_3Al_5O_{12}$ (RE=Tb, Y, Er, Yb)+1 wt% Ga_2O_3 garnet ceramics as a function of ionic radii of RE^{3+} ions.

The Claussius–Mossotti (CM) equation is used for the calculation of ε_r (CM) [23] since the ionic polarizability and unit cell volume of the rare earth garnets are known. The relative permittivity of a ceramic is very much affected by extrinsic factors such as porosity. Hence Penn et al. proposed a porosity correction factor for the relative permittivity of the material from the density of the sintered specimen [34]. The ε_r (corrected) and ε_r (CM) for $RE_3Al_5O_{12}+1$ wt% Ga_2O_3 are shown in Fig. 4. The ε_r (corrected) and ε_r (CM) shows almost same value (Fig. 4). Literature shows similar trend of relative permittivity with ionic radii of rare earth ions [5]. It has been reported that a misfit between the calculated and porosity corrected ε_r can occur due to the ionic or electronic conductivity in presence of H_2O and CO_2 channels, dipolar impurities and also due to the presence of rattling or compressed ions etc. [33].

Table 2 summarizes the sintering temperature, relative density, ε_r (corrected), ε_r (CM) and $Q_u \times f$ of the gallium oxide added rare earth aluminate garnet ceramics. It is evident that the high sintering temperature (>1600 °C) and low relative density ($\leq 92\%$) delimits the practical application of pure rare earth garnet ceramics. Hence we deliberately add Ga_2O_3 as a dopant to $RE_3Al_5O_{12}$ ceramic. The introduction of Ga_2O_3 into the matrix of $RE_3Al_5O_{12}$ could work in one of the following way: (a) even though Ga_2O_3 has a high melting point ($\sim$1740 °C), the additive can generate a low melting eutectic with one of the component of the matrix and hence enhances densification by bringing down the sintering temperature through liquid phase sintering, (b) Ga^{3+} may partly substitute at the trivalent RE^{3+} site that may result in the tilting of the oxygen polyhedra since each oxygen is a member of two dodecahedra ie, one octahedron and one tetrahedron, and (c) additive remains at the grain boundary and pin it. Also it should be noted that for 6 fold coordination, the ionic radius of Ga is 0.62 Å which is less likely to be substituted in the Al^{3+} site whose ionic radius is still smaller (0.535 Å for a coordination of 6). In the present study we observed an improvement in the densification of the garnet ceramics with the addition of Ga_2O_3 and hence one of the beneficial phenomena aforesaid is believed to have occurred (see Table 2). The composites TbAG+1 wt% Ga_2O_3 shows a relative density of 97% at sintering temperature of 1500 °C for 4 h, YAG+1 wt Ga_2O_3 shows a relative density of 95% at 1600 °C for 4 h while ErAG+1 wt% Ga_2O_3 shows 98% at sintering temperature of 1550 °C for 4 h and YbAG+1 wt% Ga_2O_3 shows 95% at 1600 °C/4 h. The dense microstructure

Table 2
Sintering temperature, relative density, ε_r (corrected), ε_r (CM), $Q_u \times f$ and τ_f of the $RE_3Al_5O_{12}$ (RE=Tb, Y, Er, Yb) with Ga_2O_3 and YAG+1 wt% Nb_2O_5 garnet ceramics.

Material	Sintering temp. (°C)	Relative density (%)	ε_r (corrected)	ε_r (CM)	$Q_u \times f$ (GHz)	τ_f (ppm/°C)
$Tb_3Al_5O_{12}+1$ wt% Ga_2O_3	1500	97	11.10	11.10	30,000	−32
$Y_3Al_5O_{12}+1$ wt% Ga_2O_3	1600	95	10.90	10.90	25,000	−33
$Y_3Al_5O_{12}+1$ wt% Nb_2O_5	1625	96	11.20	11.25	120,000	−48
$Er_3Al_5O_{12}+1$ wt% Ga_2O_3	1550	98	10.80	10.90	12,600	−37
$Yb_3Al_5O_{12}+1$ wt% Ga_2O_3	1600	97	10.50	10.70	50,000	−58

given in Fig. 2(b) and (d) also indicates that the increase in densification of the Ga_2O_3 added rare earth garnet is due to the elimination of pores probably due to liquid phase which might have enhanced the material transport [8]. The ε_r (corrected) and ε_r (CM) values are shown in Table 1, ε_r (corrected) value is in an exact agreement with the ε_r (CM). A slight variation in the value of ε_r (corrected) and ε_r (CM) are observed, this may be due to the presence of dipolar impurities and also due to the presence of rattling or compressed ions etc. [33].

It should be noted that the $Q_u \times f$ value of Ga_2O_3 doped $Tb_3Al_5O_{12}$ (30,000 GHz), $Er_3Al_5O_{12}$ (12,600 GHz) and $Yb_3Al_5O_{12}$ (50,000 GHz) are better than their intrinsic counterparts. The relatively good $Q_u \times f$ value of these rare earth garnets are due to the corresponding increase in the relative density. However, 1 wt% addition of Ga_2O_3 failed to bring about improvements in the properties of $Y_3Al_5O_{12}$ whose quality factor ($Q_u \times f$) dropped down from 65,000 GHz to 25,000 GHz after doping, the reasons for which are yet to be understood. It should be noted that 1 wt% Nb_2O_5 on YAG increases the $Q_u \times f$ value up to 120,000 GHz at a sintering temperature of 1650 °C/4 h. We found that Nb_2O_5 acts as an effective additive only in YAG and not in the case of other rare earth garnets. In the aliovalent substitution, there is an important issue of the oxygen overstoichiometry from Nb_2O_5, for which there are three plausible mechanisms likely to occur. The first one is an ionic-charge compensation mechanism in which the extra oxygen from Nb_2O_5 requires metal vacancies at either RE^{3+} or Al^{3+} sites to compensate the overcharge of Nb^{5+}. The second one is an electronic-charge compensation mechanism, in which a couple of extra oxygen ions are released and electrons are required to compensate the overcharge of Nb^{5+} at RE^{3+} sites. The last one is an oxygen vacancy filling mechanism, where a slight amount of oxygen is lost and oxygen vacancies formed during high temperature sintering in air. Both the ionic-charge compensation and the electronic charge compensation mechanisms were observed in Nb^{5+} doped TiO_2 [35].

It should be noted that the sintering temperature of Yttrium Aluminium Garnet (YAG) ceramic is 1650 °C, hence there is a possibility of creating an oxygen vacancy during the high temperature sintering. Therefore, the most possible mechanism occurring in YAG ceramic while Nb_2O_5 addition is likely to be oxygen vacancy filling mechanism. In oxygen vacancy filling mechanism, the elimination of oxygen vacancies (which are point defects) present in the lattice could be the reason for the observed high Q of the ceramic. There are several reports which clarifies the validity of the improvement of dielectric properties by the addition of Nb_2O_5 dopant as an oxygen supplier. Recently Lee et al. reported the improvement of microwave dielectric properties of $Bi_2Mo_2O_9$ by the addition of Nb_2O_5 [36]. For further clarity about the reasons responsible for the improved microwave dielectric properties of Nb_2O_5 added YAG ceramic require a detailed investigation.

Generally, τ_f value depends on the composition, additive and second phase of the material [23]. The τ_f value for the 1 wt% Ga_2O_3 added rare earth garnet composite is shown in Table 2. The τ_f values are in the range -32 to -58 ppm/°C. The good microwave dielectric and thermal properties make the rare earth garnets a good material for substrate application.

4. Conclusions

The rare earth garnet based on $RE_3Al_5O_{12}$, (RE=Tb, Y, Er, Yb) ceramics were prepared through the mixed oxide route and their structural, dielectric and thermal properties were examined. The intrinsic ceramics showed poor densification and dielectric properties when sintered at temperatures in the range 1550–1650 °C for 4 h. Hence Ga_2O_3 was added to improve the densification of $RE_3Al_5O_{12}$, however, the gallium doping was unsuitable for YAG where Nb_2O_5 was more appropriate. Among the gallium doped rare earth garnets, $Yb_3Al_5O_{12}$ $+1$ wt% Ga_2O_3 showed better dielectric properties ($\varepsilon_r=10.3$, $Q_u \times f=50{,}000$ GHz, $\tau_f=-58$ ppm/°C). However the best microwave properties were observed for $Y_3Al_5O_{12}$ garnet doped with 1 wt% Nb_2O_5 which is likely to be due to oxygen vacancy filling mechanism. In general, rare earth garnet ceramic shows low coefficient of thermal expansion (2–3 ppm/°C) and thermal conductivities are in the range 2–12 W/m K. The physical and microwave dielectric properties make rare earth aluminate garnets a suitable candidate for microwave substrate application.

Acknowledgments

The authors acknowledge the financial support from Ministry of Human Resource Development, Government of India, New Delhi. Dr. Prabhakar Rao and M.R. Chandran are also thankfully acknowledged for extending XRD and SEM facilities.

References

[1] R. Tummala, M. Kosec, W.K. Jones, D. Belavic, Electronic Packaging for High Reliability, Low Cost Electronics, Kluwer Academic Publishers, The Netherlands, Dordrecht, 1999.

[2] K. Maexa, M.R. Baklanov, D. Shamiryan, F. Iacopi, S.H. Brongersma, Z.S. Yanovitskaya, Low dielectric constant materials for microelectronics, Journal of Applied Physics 93 (2003) 8793–8841.

[3] Y. Guo, H. Ohsato, K. Kakimoto, Characterization and dielectric behavior of willemite and TiO_2 doped willemite ceramics at millimetre wave frequency, Journal of the European Ceramic Society 26 (2006) 1827–1830.

[4] L. Vasylechko, A. Senyshyn, U. Bismayer, Perovskite Type Aluminates and Gallates in Handbook on the Physics and Chemistry of Rare Earths, vol. 39, 2009, pp. 113–295.

[5] S. Thomas, M.T. Sebastian, Microwave dielectric properties of $SrRE_4Si_3O_{13}$, Journal of the American Ceramic Society 92 (2009) 2975–2981.

[6] S.Y. Cho, I.T. Kim, K.S. Hong, Microwave dielectric properties and applications of rare-earth aluminates, Journal of Materials Research 14 (1999) 114–119.

[7] M.R. Varma, N.D. Kataria, Effect of dopants on the low temperature microwave dielectric properties of $Ba(Zn_{1/3}Ta_{2/3})O_3$ ceramics, Journal of Materials Science: Materials in Electronics 18 (2007) 441–446.

[8] C.L. Huang, M.H. Weng, G.M. Shan, Effect of V_2O_5 and CuO additives on sintering behavior and microwave dielectric properties of $BiNbO_4$ ceramics, Journal of Materials Science 35 (2000) 5443–5447.

[9] M.T. Sebastian, H. Jantunen, Low loss dielectric materials for LTCC applications, a review, International Materials Reviews 53 (2008) 57–90.

[10] J. Lu, K. Ueda, H. Yagi, T. Yanagitani, Y. Akiyama, A.A. Kaminskii, Neodymium doped yttrium aluminum garnet ($Y_3Al_5O_{12}$) nanocrystalline ceramics a new generation of solid state laser and optical materials, Journal of Alloys and Compounds 341 (2002) 220–225.

[11] J. Krupka, K. Derzakowski, M. Tobar, J. Hartnett, R.G. Geyer, Complex permittivity of some ultra loss dielectric crystals at cryogenic temperatures, Measurement Science and Technology 10 (1999) 387–392.

[12] N.F. Vedernikov, A.K. Zvezdin, R.Z. Levitin, A.I. Popov, Magnetic linear birefringence of rare-earth garnets, Zhurnal Eksperimental′noi i Teoreticheskoi Fiziki 93 (1987) 2161–2178.

[13] L. Gao, F. Gao, Chemical bond properties and hardness estimation of rare earth garnets, Materials Chemistry and Physics 113 (2009) 145–149.

[14] S. Hosokawa, Y. Tanaka, S. Iwamoto, M. Inoue, Defect structure of rare earth aluminum garnets obtained by the glycothermal method, Journal of Alloys and Compounds 451 (2008) 309–313.

[15] M. Vlasova, M. Kakazey, B. Sosa Coeto, P.A. Marquez Aguilar, I. Rosales, A.E. Martinez, V. Stetsenko, A. Bykov, A. Ragulya, Laser synthesis of Al_2TiO_5 and $Y_3Al_5O_{12}$ ceramics from powder mixtures Al_2O_3–TiO_2 and Al_2O_3–Y_2O_3, Science of Sintering 44 (2012) 17–24.

[16] I. Kagomiya, Y. Matsuda, K. Kakimoto, H. Oshato, Microwave dielectric properties of YAG ceramics, Ferroelectrics 387 (2009) 1–6.

[17] Y. Zhou, Z. Yue, L. Li, Preparation and microwave dielectric properties of TiO_2 doped YAG ceramics, Ferroelectrics 407 (2010) 69–74.

[18] J.I. Yang, S. Nahm, C.H. Choi, H.J. Lee, J.C. Kim, H.M. Park, Effect of Ga_2O_3 on microstructure and microwave dielectric properties of $Ba(Zn_{1/3}Ta_{2/3})O_3$ ceramics, Japanese Journal of Applied Physics 41 (2002) 702–706.

[19] H.M. Shirey**,** Low Temperature Synthesis of the Microwave Dielectric Material, Barium Magnesium Tantalate (BMT), (Master′s thesis), University of Pittsburgh, USA, 2003.

[20] A. Feteira, K. Sarma, N.M. Alford, I.M. Reaney, D.C. Sinclair, Microwave dielectric properties of gallium doped hexagonal barium titanate ceramics, Journal of the American Ceramic Society 86 (2003) 511–513.

[21] B.W. Hakki, P.D. Coleman, A dielectric resonator method of measuring inductive capacities in the millimeter range, IEEE Transactions on Microwave Theory and Techniques 8 (1960) 402–410.

[22] J. Krupka, Fequency domain complex permittivity measurements at microwave frequencies, Measurement Science and Technology 17 (2006) R55–R70.

[23] M.T. Sebastian, Dielectric Materials for Wireless Communication, Elsevier, Oxford, UK, 2008.

[24] H. Shibata, A. Suzuki, H. Ohta, Measurement of thermal transport properties for molten silicate glasses at high temperatures by means of a novel laser flash technique, Materials Transactions 46 (2005) 1877–1881.

[25] Y.N. Xu, W.Y. Ching, Electronic structure of yttrium aluminum garnet $Y_3Al_5O_{12}$, Physical Review B 59 (1999) 10530–10535.

[26] B.D. Cullity, Elements of X-ray Diffraction, second ed., Addision-Wesely Publishing Company, USA, 1978.

[27] K.P. Surendran, S. Solomon, M.R. Varma, P. Mohanan, M.T. Sebastian, Microwave dielectric properties of $RETiTaO_6$ (RE=La, Ce, Pr, Nd, Sm, Eu, Gd, Tb, Dy, Ho, Y, Er, Yb, Al, and In) ceramics, Journal of Materials Research 17 (2002) 2561–2566.

[28] L.A. Khalam, M.T. Sebastian, Microwave dielectric properties of $Sr(B'_{1/2}Nb_{1/2})O_3$ [B′=La, Pr, Nd, Sm, Gd, Tb, Dy, Ho, Y, Er, Yb and In] ceramics, International Journal of Applied Ceramic Technology 3 (2006) 364–3674.

[29] A. Kareiva, Aqueous sol–gel synthesis method for the preparation of garnet crystal structure compounds, Materials Science 17 (2011) 428–437.

[30] E. Garskaite, S. Sakirzanovas, A. Kareiva, J. Glaser, H.J. Meyer, Synthesis and structure of europium aluminum garnet (EAG), Zeitschrift fuer Anorganische und Allgemeine Chemie 633 (2007) 990–993.

[31] J.H. Park, B.K. Kim, J.G. Park, Y. Kim, Effect of microstructure on the microwave properties in dielectric ceramics, Journal of the European Ceramic Society 21 (2001) 2669–2672.

[32] W.D. Kingery, Introduction to Ceramics, John Wiley and Sons, New York, 1960.

[33] R.D. Shannon, Dielectric polarizabilities of ions in oxides and fluorides, Journal of Applied Physics 73 (1993) 348–366.

[34] S.J. Penn, N.M. Alford, A. Templeton, X.R. Wang, M.S. Xu, M. Reece, Effect of porosity and grain size on the microwave dielectric properties of sintered alumina, Journal of the American Ceramic Society 80 (1997) 1885–1888.

[35] J.F. Baumard, E. Tani, Electrical conductivity and charge compensation in Nb doped TiO_2 rutile, Journal of Chemical Physics 67 (1977) 857–860.

[36] Y.C. Lee, J.D. Chiu, Y.H. Chen, Effect of Nb_2O_5 doping on the microwave dielectric properties and microstructure of $Bi_2Mo_2O_9$ ceramics, Journal of the American Ceramic Society 96 (2013) 1477–1482.